

## The Electrical properties of sintered compacts of BiSnSe<sub>2</sub>.

M. M. Abd El-Raheem, M. M. Ibrahim, A. M. Ahmed,  
S. A. Ahmed

Department of Physics, Faculty of Science, Sohag, EGYPT

*The prepared samples of BiSnSe<sub>2</sub> using cold pressing technique showed semimetallic and semiconductor behavior depending on the conditions of sintering. Among the semiconductor behavior, the resistivity is weakly dependent on the ambient temperature which is owed to the hopping mechanism to conduction. Also, the behavior of the electrical properties with the applied electric field and the ambient temperature have been detected and interpreted as due to intergrain and intragrain coupling.*

### 1. Introduction:

IV-VI semiconductor such as Pb Te, Pb Se, Sn Se, or Sn Te are strongly degenerated materials with a narrow gap [1983]. The characteristic property of these crystals is a very high concentration of vacancies in such materials, there exists a possibility to control the number of vacancies by an isothermal annealing [1997]. The electrical conductivity and Seebeck coefficient of samples with various of ternary compounds in the SbTe-Bi<sub>2</sub>Te<sub>3</sub> system show that the transport properties strongly vary with composition and temperature [2003].

Number of binary liquid chalcogenide alloys of the system IV – VI have been found to show semiconductor – metallic transition with the change of composition and temperature, [1969]. Sn – Se alloy in the solid state contains two intermediate compounds Sn Se and Sn Se<sub>2</sub>, both of which melt congruently, [1992].

Semiconductor with a narrow forbidden gap have a high static dielectric constant of the lattice. Which generally consists of a phonon and electron contributions, (Rudolph et al [1980]), (Z Zhang [2000]). However, such materials containing Bi are expected to possess narrow forbidden gap that is because of the semimetallic behaviour of these materials. In addition, the

gapless semiconductor could be observed in Bi based alloys and could be attributed to overlapping of valence and conduction bands, Ibrahim et al [1980]. Solid solutions on the basis of narrow layered semiconductors  $A_2^V B_3^{VI}$  (where  $A = \text{Bi Sb}$  and  $B = \text{Se, Te}$ ) of tetradymite structure (space group  $D_{3d}^{5}$ ) find applications in the field of thermoelectric devices (Birkholz [1984]). Besides, solid solutions formed by the melting of  $\text{Bi}_2\text{Te}_3$  and  $\text{Bi}_2\text{Se}_3$  (two  $A_2^V B_3^{VI}$  binaries) are well known to be the best n-type materials for thermoelectric refrigeration at room temperature, and therefore a great amount of work has been done on these alloys, including different methods of preparation. Also, considerable attention has been focused on glassiness of Bi and Se because of their use in optical and photosensitive devices (Bates and England [1969]). The question arised in suggesting the present work was a wondering about the situation of substituting Te by its isomar (Se) in the system to study the physical properties of Bi - Sn - Se ternary alloy, prepared by quite different method as will be discussed latter on.

It was found that thermoelements prepared by sintering having the compositions  $\text{Bi}_{0.5}\text{Sb}_{1.5}\text{Te}_3$  with 0.05 mass % Pb are p – type and  $\text{Bi}_2\text{Te}_{2.7}\text{Se}_{0.3}$  with 0.2 mass % S are n – type ( Ibrahim et al [1988]. Yokota and Katayama [1975] found the p – type  $\text{Bi}_2\text{Te}_3$  compound changes to n – type after short time of sintering at 400 and 500 °C, respectively. Also, controlling the green density, particle size, time and temperature of sintering was found essential to obtain powder compacts of the system  $\text{Bi}_{1-x}\text{Te}_x$  with controlled physica properties Ibrahim et al [1988].

## 2. Experimental Technique:

The ternary  $\text{BiSnSe}_2$  cast alloy was prepared by using the traditional melt quench technique. The precursor elements were Bi 99.999%, Sn99.999 and Se 99.999. The resulted bulk ingot has been grinded thoroughly using an agate mortar and then a 63  $\mu\text{m}$  particle size has been obtained using electrical shaker. Samples in powder compact form have been prepared using cold pressing technique.

The current (I) – voltage(V) measurements were carried out in the range  $93 \leq T \leq 393\text{K}$  using a conventional sereis circiut with pressure contact holder under moderate vacuum up to  $10^{-3}$  mmHg. The electrical resistivity  $\rho$  was measured using the Van der Pauw technique. The x – ray investigation has been carried out using a philips diffractometer (type 1710) with  $\text{CuK}_\alpha$  target and graphite monochromator giving a monocromatic beam with wave length 1.5418 °A at 40v and 30mA with scanning speed of 3.76 deg/min.

The surface microstructure of the tested specimens were examined using a scanning electron microscope type  $J_s M - 5300$ (Japan). In order to stydy

the surface morphology of a specimen, it must be highly polished and with clean surface.

### 3. Results and discussions:

#### The current density (J) – Electric field (E) characteristics

The J–E characteristics of the green compact of the  $\text{BiSnSe}_2$  were traced at different temperatures in the range from 93 to 333K are as shown in Fig.(1-a). The first glimpse to those characteristics reveal the possibility of Ohmic – nonOhmic transition at all considered temperatures of measurements. It is obvious from Fig.(1-a) that J increases with increasing T i.e the series current can be thermally activated. Also, at a certain applied potential, which can be called as the turn – over potential ( $V_t$ ). The ratio  $dI / dV$  increased abruptly indicating that, the as – prepared sample of  $\text{BiSnSe}_2$  can undergo switching.

Similar behaviour could be observed for the compact sintered at 250, 325, and at 400C for different periods of time 5, 10, 20, 320 and 640 mins. As shown in Fig.(1-b) for  $T_s = 400^\circ\text{C}$  and  $t_s = 640$  mins. As an example.

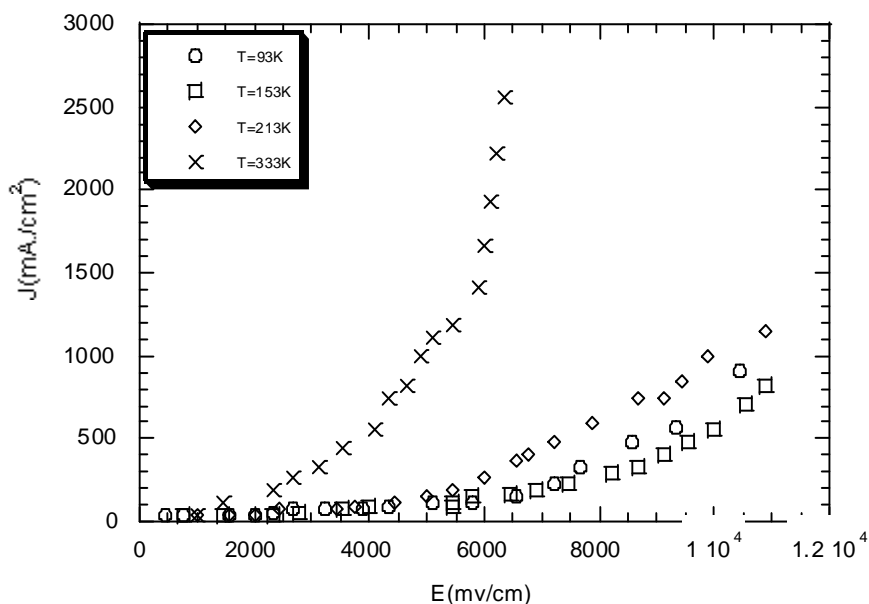
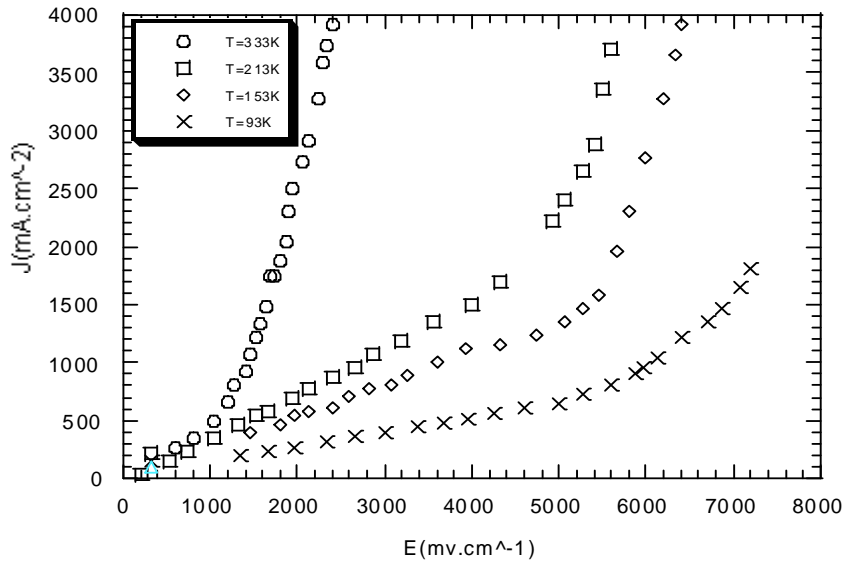
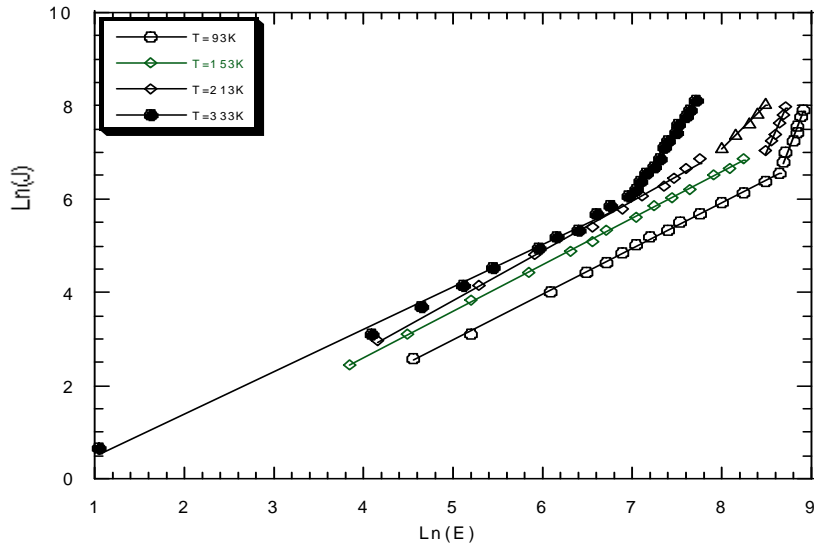


Fig.(1-a):Variation of J vs. E for green compact.



**Fig. (1-b):** Variation of J vs.E sintered compacts at  $T_s = 100^\circ\text{C}$  and  $t_s = 640$  mins. at different T (k).

The double logarithmic plots between J and E for green and sintered compacts where drawn as seen in Fig.(2) as an example of the case  $T_s = 400^\circ\text{C}$  for  $t_s = 640$  mins.



**Fig. (2):** Variation of Ln(J) vs. Ln(E) for compacts sintered at  $T_s = 400^\circ\text{C}$  and  $t_s = 640$  mins. at different T (k).

The  $\ln J - \ln E$  plots were found to be multistage, each stage is characterized by its own slope  $n$  follow the equation  $J = C E^{n(T)}$  where  $n$  is dependent on both the environmental temperature and the applied field. In addition, every two successive ranges of  $J - E$  dependence is separated by a transition field  $E_r$ . The values of  $E_r$  and  $n$  were calculated and tabulated in table (1&2) for as-prepared and sintered at 325C and 400C respectively.

**Table(1):** Variation of the power  $n$  and  $E_r$  with  $t_s$  at  $T_s = 325^\circ \text{C}$ .

$T_{am. (K)}$	153	213	333
green			
$(n_1)$	0.995	1.068	0906
$(n_2)$	3.628	2.749	2.5477
$E_r(\text{v/cm})$	7.230	5.380	3.3930
$T_s = 20 \text{ mins}$			
$(n_1)$	1.1606	1.2323	1.1397
$(n_2)$	2.4853	1.5922	2.0596
$E_r(\text{v/cm})$	3.5870	3.6370	1.3370

**Table(2):** Variation of the power  $n$  and  $E_r$  with  $t_s$  at  $T_s = 400^\circ \text{C}$ .

$T_{am}(K)$	153	213	333
$T_s = 20 \text{ mins.}$			
$(n_1)$	1.061	1.0513	1.0183
$(n_2)$	1.264	2.348	1.1598
$E_r(\text{V/cm})$	1.401	3.101	0.785
$T_s = 320 \text{ mins.}$			
$(n_1)$	1.199	1.199	1.0871
$(n_2)$	2.327	1.932	2.438
$E_r(\text{V/cm})$	4.218	2.579	1.227
$T_s = 640 \text{ mins.}$			
$(n_1)$	1.017	1.063	0.934
$(n_2)$	4.597	2.832	2.559
$E_r(\text{V/cm})$	5.11	4.222	0.903

At these tables, for green and sintered compacts for 20 mins.,  $n_1$  corresponds to the lowest range of  $E$  and possessed a value near to unity confirming that, at relatively weak applied electric field, ohmic conduction behaviour is prevailing in both cases, green and sintered compacts. On the other hand,  $n_2$  which correspond to the higher range of  $E$  exceeded much the

value unity confirming that the Omic behaviour is no longer valid and the conductivity  $\sigma = J / E$  became field dependent .

The  $\ln\sigma$ -E are drawn for the green and sintered compacts at the considered temperature and time of sintering. As shown in Fig.(3-a&b), the plots of  $\ln \sigma(E)$  vs. E at different ambient temperatures in the range  $93 \geq T \geq 333$  for sintered compact at 325 °C for 40 mins and sintered one at 400 °C for 640 mins are linear and may follow the equation [1973];

$$\sigma ( E ,T) = \sigma ( E ,0) \exp [ ea (T).E / KT] \quad (1)$$

where E is the applied electric field, a(T) is a temperature dependent parameter having the dimintions of length,  $\sigma ( 0,T)$  is the field independent conductivity at particular temperature, e is the electronic charge and K is the Boltzmann's constant.

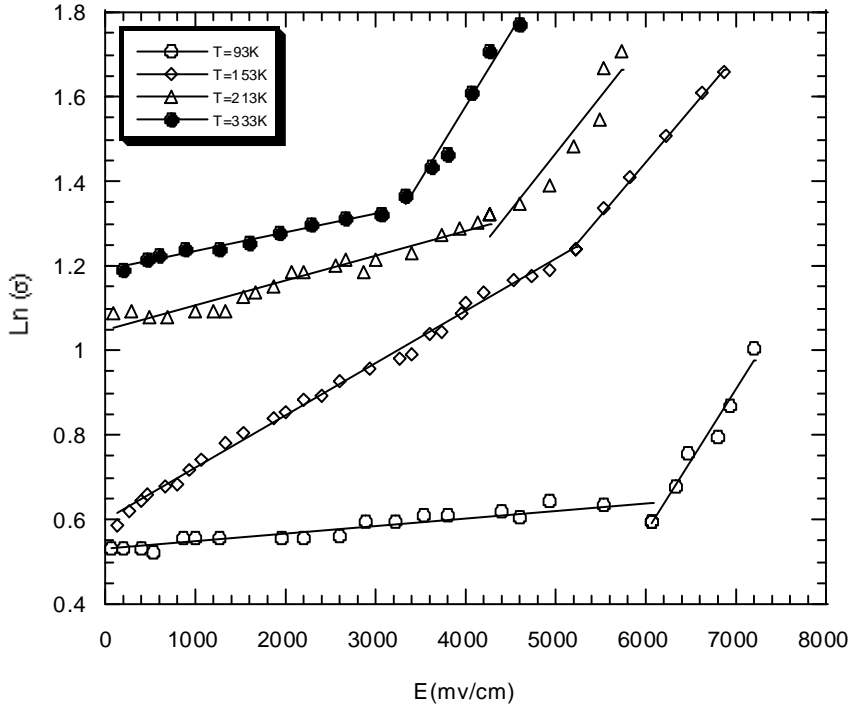


**Fig. (3-a):** Variation of Ln(ε) vs. E for sintered compact at Ts = 325C and ts = 40 mins.

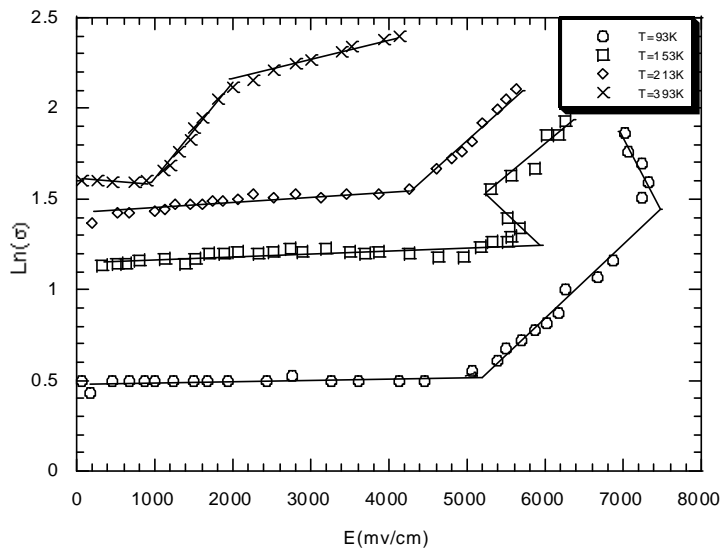


Fig.(3-b):Variation of  $\text{Ln}(\sigma)$  vs.  $E(\text{mv/cm})$  for sample sintered at  $T_s = 400\text{C}$  and  $t_s = 640$  mins at different  $T(\text{K})$ .

Fig.(3-a) shows that  $\sigma$  depends on the range of  $E$ . On the other hand Fig.(3-b) shows another behaviour, where, the general feature of the considered plot is characterized by whether a weak dependence or entire independency of  $\ln \sigma(E)$  on  $E$  which represents the Ohmic behaviour. The highest range of  $E$  characterized by multi-feature dependence of  $\ln \sigma(E)$  on  $E$  that is because of the possibility of the turn – over or switching process as discussed in the former section. However, the most important are those regions characterized by conductivity field enhancement, since it gives the possibility of calculating the parameter  $a(T)$ . Further, the field independent conductivity  $\sigma(0,T)$  can be determined from the extrapolation of this region. Thus, both  $a(T)$  and  $\sigma(0,T)$  were calculated, at different times of sintering, at particular temperature. The obtained results indicated regular dependence of both  $\sigma(0,T)$  and  $a(T)$  on the temperature of measurement. The double logarithmic relations of both  $\sigma(0,T)$  and  $a(T)$  vs.  $T$  were plotted. This was a trial to generalize the temperature dependence of  $\sigma(0,T)$  and  $a(T)$ .

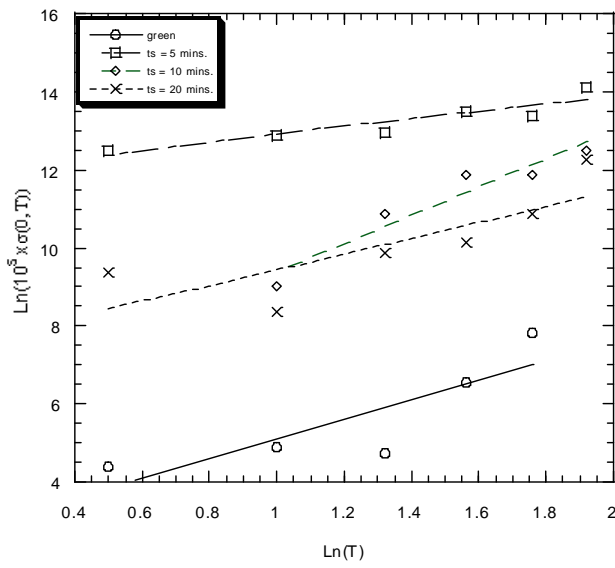


Fig.(4-a): Variation of  $\text{Ln}(\sigma(0,T))$  vs.  $\text{Ln}(T)$  for green and sintered sample at  $T_s = 325^\circ\text{C}$  at different  $t_s$ .

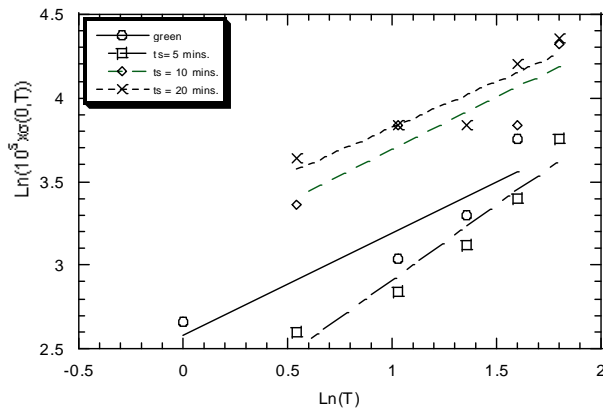


Fig.(4-b): Variation of  $\text{Ln} \alpha(0,T)$  vs.  $\text{Ln}(T)$  for green and sintered compacts at  $400^\circ\text{C}$  at different  $t_s$ .

As it is seen in Figs.(4-a&b), the plots of  $\ln \sigma (0,T)$  vs  $\ln T$  are linear, suggesting the possibility of describing the dependence in terms of a power equation as

$$\sigma ( 0,T) \sim T^y \tag{2}$$

Meanwhile, Fig. (5) represents  $\ln a(T)$  vs.  $\ln (T)$  suggests the following power equation;

$$\alpha(T) \sim T^\zeta \tag{3}$$



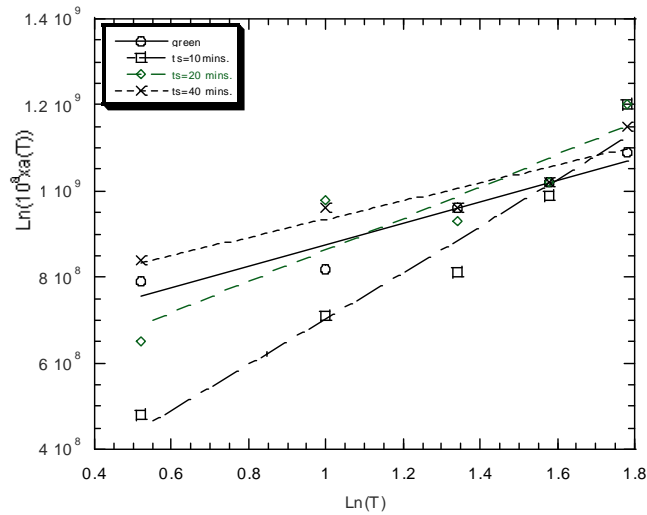


Fig.(5): Variation of Ln a(T) vs. Ln(T) for green and sintered compacts at Ts=325C at different ts.

Both the powers y and z are calculated and their dependencies on the time of sintering are recorded in table (3).

**Table (3):** Variation of z and y with ts and Ts .

ts (mins.)	z	ts (mins.)	y	Ts
00.00	1.7935	0.000	1.6593	325°C
10.00	1.6469	10.00	1.7562	
20.00	1.5622	20.00	0.9728	
-----	-----	-----	-----	-----
-	-	-	-	400°C
10.000	0.4816	10.000	0.54220	
20.000	3.6392	20.000	1.11665	

As it is seen in table (3), the powers y and z have a trend to decrease with increasing the time of sintering at both considered sintering temperatures.

It is clear from equation (1) that the product a(T).E gives the potential difference of the electrical work required for charge carrier transportation to contribute to the observed electrical conductivity at a particular temperature of measurement. Consequently, the significance of a(T) can be understood to be

the distance should a charge carrier travel to contribute to conduction. In case of non-crystalline solids it is acceptable to be related to the hopping distance. In case of the granular materials such as the powder compacts, it is acceptable to be related strongly to the potential barriers due to the boundaries between the grains. However, this explanation seems controversial since,  $a(T)$  was found to increase with increasing  $T$ . Therefore, it is more logic to correlate the increase in  $a(T)$  with  $T$  to a corresponding thermal activation of the processes of scattering. In turn,  $a(T)$  should be correlated to the mean free path and the frequency of collision process occurred during the transition of charge carrier from one site to another along the compact dimentions. As it is seen in Fig(6), the plots of  $\ln \sigma(0,T)$  vs  $1 / T$  are linear with minus coefficient suggesting the following empirical formula;

$$\ln \sigma(0,T) = C \exp [ - \Delta E_{\sigma}( 0, T ) / KT ] \quad (4)$$

Wher  $C$  is a temperature independent parameter having the significance of the temperature independent zero field electrical conductivity and  $\Delta E$  has the significance of an activation energy. i . e the energy required for thermal activation of  $\sigma(0, T)$ .

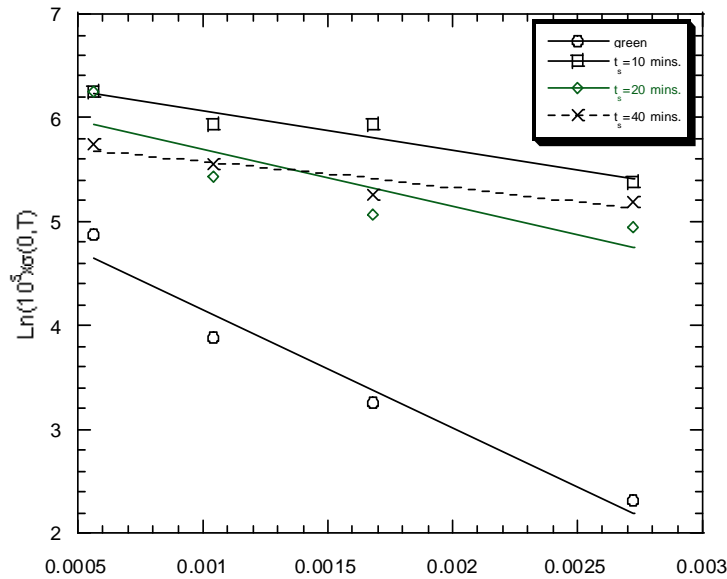


Fig.(6): Variation of  $\ln \sigma$  vs.  $(1/T)K^{-1}$  for green and sintered compacts at  $T^s = 325 \text{ }^\circ\text{C}$  at different  $t_s$ .

**Table (4) :** Variation of  $\Delta E_{\sigma(0,T)}$  and  $\Delta E_{a(T)}$  with  $t_s$ (mins.) and  $T_s$ .

$t_s$ (mins.)	$\Delta E_{\sigma(T)}$ (e.v)	$t_s$ (mins.)	$\Delta E_{a(T)}$ (e.v)	$T_s$
00.00	0.02708	0.000	0.02182	325°C
10.00	0.03410	10.00	0.03623	
20.00	0.02506	20.00	0.01211	
40.00	0.01331	40.00	0.00538	
-----	-----	-----	-----	-----
10.000	-	10.000	0.00814	-
20.000	0.00530	20.000	0.01481	400°C
40.000	0.04871	40.000	0.01823	
	0.03092			

As it is seen in table (4),  $\Delta E_{\sigma}(0,T)$  decreased with increasing sintering time at 325 °C except at  $t_s = 10$  mins.. Also, at  $T_s = 400$  ° C,  $\Delta E(0, T)$  showed the same trend of change with  $t_s$  as the power  $z$  in equ.(3).

On the other hand, it was found that the  $\ln a(T)$  vs.  $1/T$  plots were also linear, suggesting similar exponential empirical equation to describe the temperature dependence of  $a(T)$  as follows;

$$a(T) = C \exp [ - \Delta E_a(T) / KT ] \quad (5)$$

Where  $C$  is a temperature independent constant representing the value of  $a(T)$  at infinite temperature.  $\Delta E_{a(T)}$  is the corresponding activation energy having the significance of the energy required for thermal elongation of the distance between two successive sites of the charge carriers as discussed above. As it is seen in table (4),  $\Delta E_{a(T)}$ , possessed small values and having the same trend with  $t_s$  as for the power  $z$  in equ.(3).

The question arises now is , to what extent,  $\Delta E_{a(T)}$  can be compared to the hopping energy. The answer will be presented later on.

#### 4. Electrical Resistivity:

Tracing the temperature dependences of resistivity revealed the possibility of semiconductor, metallic and semiconductor – metallic transition behaviours. This is found to depend on the temperature and time of sintering and also the range of temperature at which the resistivity was measured. The linear scale temperature dependence of the resistivity in the range  $183 \leq T \leq 383K$  for the green and sintered for different times at 250, 325 and 400 ° C

compacts indicated the possibility of prevailing of the three types of behaviours as mentioned above. Therefore, it seemed more convenient to separate each behaviour and treat it separately. Fig.(7) shows the double logarithmic relations between the resistivity ( $\rho$ ) and the temperature of measurement where the behaviour proved to be semimetallic which can be described by the following equation;

$$\text{Ln}(\rho - \rho_0) = \alpha \text{Ln} T \quad \text{or} \quad \rho = \rho_0 + T^\alpha \quad (6)$$

Where  $\rho_0$  has the significance of the residual resistivity. As shown in table (5),  $\rho_0$  found to depend on the temperature  $T_s$  as will as  $\alpha$ .

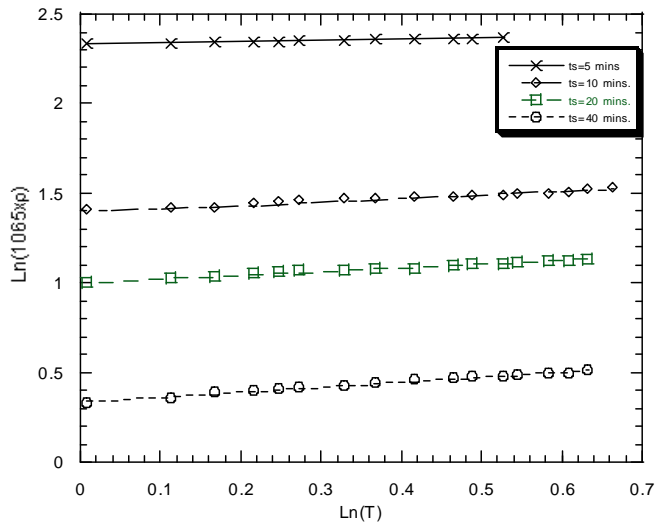


Fig.(7) Ln( $\rho$ ) vs. Ln(T) for green and sintered compacts at  $T_s=250\text{C}$  at different  $t_s$

**Table (5) :** Variation of  $\alpha$  and  $\rho_0$  ( $\Omega\cdot\text{cm}$ ) with  $t_s$  (mins.) and  $T_s$ ( $^\circ\text{C}$ )

$t_s$ (mins.)	$\alpha$	$\rho$	$T_r$ (K)	$T_s$ ( $^\circ\text{C}$ )
40.00	0.0728	10.6579	-----	250
40.00	0.01350 0.08550	12.8010 8.6167	244 -----	325
40.00	0.13700 0.19000	6.3994 4.7803	245 354	400

	0.05100	10.8090	-----	
--	---------	---------	-------	--

It is seen also in table (5) that  $\alpha$  increases with increasing  $T_s$  (considering the second stage belongs to  $T_s = 325$  °C), whereas,  $\rho_o$  behaved inverse to that of  $\alpha$ .

Also, It is observed also from table (5) that the sintered compact at 325 °C has a metallic behaviour at 40 mins. of sintering. Further, Sintering at 400 °C results in values of  $\rho_o$  comparable to those of pure metals as indicated in table (5). The relation between  $\ln\sigma$  and  $1/T$  found to be linear possessing negative sign slopes and follow the equation;

$$\sigma = \sigma_o \exp [ - \Delta E_\sigma / KT ] \tag{7}$$

The values of the conduction activation energy corresponding to these slopes were as recorded in table (6). It is clear from table (6) that  $\Delta E_\sigma$  increased by transition from one lower stage to the successive highr one of T, on the other hand, the values of  $\Delta E_\sigma$  are small, in the range of millielectronvolt, so in the basis of the small values of  $\Delta E$ , the weak dependence of  $\sigma$  on T can be emphasized.

Table (6): Variation of  $\Delta E_\sigma$ (e.v),  $\sigma_o(\Omega.cm)^{-1}$  and  $T_r(K)$  with  $t_s$  and  $T_s$ .

$t_s$ (mins.)	$\Delta E_{\sigma 1}$ (e.v)	$\Delta E_{\sigma 2}$ (e.v)	$\Delta E_{\sigma 32}$ (e.v )	$\sigma_o 1(\Omega.CM)^{-1}$	$\sigma_o 2(\Omega.CM)^{-1}$	$\sigma_o 3(\Omega.CM)^{-1}$	Tr1(K)	Tr1(K)
$T_s = 250$ °C								
0.00	-0.01470	-0.03510	-0.0877	284.80	728.2	4972.7		251.60
318.15								
80.0	-0.00166	-0.00996	-----	8558.0	11421	-----		333.33
-----								
$T_s = 325$ °C								
0.00	-0.0138	-0.04250	-0.1006	170.80	671.6	6353.2		243.60
299.90								
80.0	-0.0072	-----	-----	9041.6	-----	-----		-----
-----								

Also, it is observed from table (6) that  $\sigma_o$  behaved similar to  $\Delta E_\sigma$ , despite, it possessed small values especially these corresponding to the lowest range of T. This is another confirmation of the weak dependence of the electrical conductivity on temperature. This weak dependence of resistivity on temperatures promotes thinking about hopping conduction which was tested in the following. Considering that the measured conductivity  $\sigma$  is a sum of  $\sigma_{Ext}$

(band – type conduction) and  $\sigma_{\text{hop}}$  (due to hopping conduction within the localized states), Mott [1971] proposed the following expression to describe the temperature dependence of the hopping conductivity,

$$\sigma_{\text{hop}} = \sigma T^{-1/2} \exp [ -(T / T_0)^{1/4} ] \quad (8)$$

where  $\sigma_0^2 \sim [ N(E_F) / 2\pi \alpha K ] \{ 3e^2 v \phi_0 / 2 \}$  (9)

where  $v$  is the Debye frequency ( $\sim 10^{13}$  Hz) (Nagels [1980]) and  $e$  is the electronic charge and  $\phi_0$  is an overlap integral and is of the order of unity.

The density of states  $N(E_F)$  at the Fermi level can be calculated on considering the value of  $T_0$  which represents the slope of the  $\ln(\sigma T^{1/2})$  vs.  $T^{-1/4}$

Since  $T_0 = 18 \gamma^2 / K_B N(E_F)$  (10)

The parameter  $\gamma$  in the above equation represents the coefficient of exponential decay of the localized state and assumed to be  $0.124 \text{ } ^\circ\text{A}^{-1}$  (Fritsche [1974]). On the other side, the hopping distance can be expressed as follows;

$$R = \{ 9/8 \pi \gamma K_B T N(E_F) \}^{1/4} \quad (11)$$

And can be calculated at different conditions. Furthermore the average hopping energy  $W$  could be also calculated using the following expression;

$$W = 3/4 \pi R^2 N(E_F) \quad (12)$$

The linear plots between  $\ln(\sigma T^{1/2})$  and  $T^{-1/4}$  proved the possibility of application of Mott's formula for hopping conductivity. The corresponding Mott's parameters are calculated and then recorded in table (7).

As seen in table (7), three ranges of dependence of  $\sigma T^{1/2}$  on  $T^{-1/4}$  could be observed in case of green compacts. Consequently, three values could be calculated for each of the Mott parameters. Those parameters were calculated first for three green compacts which were post – sintered at the considered three temperatures 250, 325, and 400 ° C. The slight deviation in different Mott parameters from compact to another indicates the sampling effect which could be ignored any how. However, this very slight differences proved good control in the conditions of preparation.

As shown in table (7), the values of  $\sigma_0$  belonging to the three green compacts decreases with transition from lower to successive higher range of  $T$ . This proved more thermal activation of the electrical conductivity with increasing the range of temperature i.e the hopping conduction is thermally assisted. Meanwhile,  $T_0$  increased with transition from a lower to a successive

higher range of T, this confirms again thermally activated conduction or thermally assessed hopping conduction. On the other hand, values of  $N(E_F)$  decrease with elevating the range of T, such behaviour confirms the possibility of contribution of band to band (extended states) conduction at elevated temperature ranges. Besides, the hopping distance R, possessed values ranging from  $10^{-7}$  to  $10^{-6}$  cm and increase with increasing T. These values of R are very small with respect to the average particle size of the originally compacted powder. Also, they are very small with respect to the inter particle distance. This might indicate that hopping occurs mainly between the localized states in the grains themselves i.e intragrain hopping. The contribution of hopping between the particles themselves which can be called as intergrain hopping (hopping between grain boundaries i.e between the particles constituting the compact) can not be ignored, however, its role seems weak. On the other hand, the average hopping energy W for green compacts possessed very small values, and its value increased with elevating T.

**Table (7) :** Variation of Mott's parameters with  $T_s(^{\circ}\text{C})$  and  $t_s(\text{mins.})$

$T_0(\text{K})$	$N(E_F)\text{ev}^{-1}\text{cm}^{-3}$	$\sigma_0 \times 10^4 (\Omega\text{cm})^{-1}$	R(cm)	$W \times 10^3 \text{ev}$	$t_s(\text{mins.})$	$T_s(^{\circ}\text{C})$
181801.00	2.19E+21	3.540	6.25E-7	0.446		
1637102.0	2.43E+20	1.180	1.08E-6	0.772		green
18165763	2.19E+19	0.354	1.98E-6	1.409		
7179.0	2.55E+22	17.82	2.79E-7	0.199	80	250
41945	9.5E+21	7.37	4.33E-7	0.309		
178201	2.23E+21	3.580	6.22E-7	0.443		
5008854	7.95E+19	0.675	1.43E-6	1.021		green
50172321	7.94E+18	0.213	2.55E-6	1.816		
26839	1.48E+22	9.220	3.88E-7	0.376	80	325
56216	7.08E+21	6.370	4.66E-8	0.332		

Considering that this energy is that required for hopping to occur, these small values reveal easy hopping. This is a consequences of the relatively small values obtained for the hopping distance R. Regarding the values of R and W in table (7) it is obvious that W is directly proportional to R. Meanwhile, the values obtained for W are about one order of magnitude smaller with respect to the values obtained for  $\Delta E_{\alpha(T)}$  recorded in table (4). This may reveal that not only intergrain but intragrain hopping is contributing to the total hopping process occurring in the sample.

As mentioned before, sintering at  $250^{\circ}\text{C}$  was characterized by semimetallic behaviour except at 80 mins. of sintering. Despite of this unique

time of sintering at which hopping conduction was prevailing, the different Mott parameters were calculated and then recorded in table (7). As it is seen, the process of sintering at this temperature for this period of time, resulted in promptness of the extrapolated conductivity  $\sigma_0$  by about one order of magnitude. The corresponding value for  $T_0$  decreased while  $N(E_F)$  increased by about one order of magnitude. The hopping distance possessed values in the ranges of  $10^{-7}$  at both ranges of  $T$ . Consequently, the average hopping energy possessed relatively small values compared to the green condition.

At  $325^\circ\text{C}$  of sintering, hopping condition was prevailing and the corresponding Mott parameters are as seen in table (7).

At  $T_s = 325^\circ\text{C}$ , the characteristic temperature  $T_0$  possessed values in the ranges  $10^5 - 10^4$  where hopping conduction was prevailing.

The density of localized states  $N(E_F)$  has values in the range of  $10^{22}\text{ cm}^{-3}\text{ eV}^{-1}$ . The hopping distance  $R$  possessed values in the range  $10^{-7}\text{ cm}$  and the general trend of  $R$  is to decrease with prolongating  $t_s$ .

As a whole, the general trend is that,  $R$  increased with decreasing  $T_s$ .  $W$  changed parallel to  $R$  since both decreased with prolongating  $t_s$ .

The effect of sintering time at  $T_s = 250^\circ\text{C}$  and  $400^\circ\text{C}$  could be revealed by plotting the normalized change in the resistivity  $\epsilon$  as a function of  $t_s$  as shown in Fig.(8).

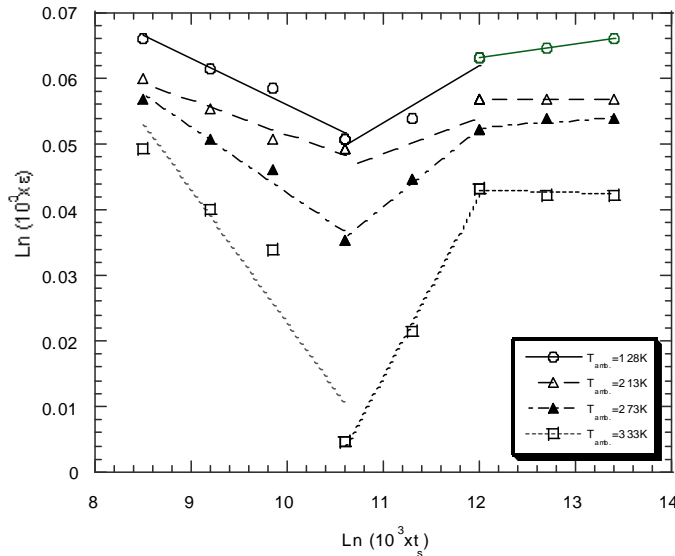


Fig.(8-a):  $\text{Ln}(\epsilon)$  vs.  $\text{Ln}(t_s)$  for sintered compact at

$T_s = 250^\circ\text{C}$  at different ambient temperatures.



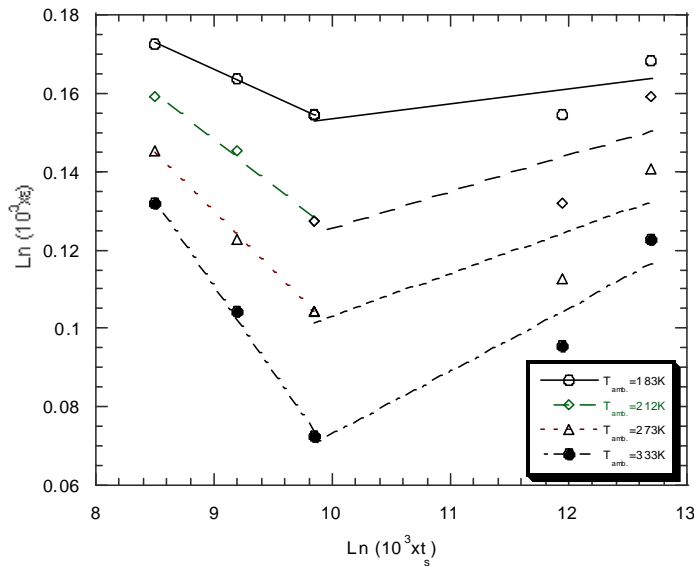


Fig.(8-b): Ln (ε) vs. Ln (t) for sintered compact at  $T_s = 400^\circ C$  at different ambient temperatures.

As it is seen in the later figure, the first small period of sintering is characterized by a decrease in  $\epsilon$  by prolongating  $t_s$ . However, it is worth mentioning that the normalized change in resistivity  $\epsilon = (\rho_{ts} - \rho_0) / \rho_0$  where,  $\rho_0$  is the resistivity of the green compact and  $\rho_{ts}$  is that measured at particular time of sintering. As it is shown that  $\epsilon$  possessed minimum value at  $t_s = 40$ , and 20 at  $T_s = 250^\circ C$  and  $400^\circ C$  respectively. Above these times,  $\epsilon$  increased again with further prolongating  $t_s$ . Another minima could be observed at  $t_s$  160 mins. for  $T_s = 400^\circ C$ .

The linear dependence of  $\ln \epsilon$  on  $\ln t_s$  is found to follow the power equation;

$$\epsilon = C t^{\pm\alpha(T)} \tag{13}$$

As formally mentioned that the power  $\alpha$  possessed wether plus or minus sign depending on wether  $\epsilon$  increases or decreases with prolongating  $t_s$ . Values calculated for  $\alpha$  are recorded in table (8).

As it is seen at  $T_s = 250^\circ C$ , three values were recorded for  $\alpha$  which are corresponding to the three linear parts of each of the double logarithmic plots. It is obvious that  $\alpha_1$  and  $\alpha_2$  increases with increasing the ambient temperature,

whereas,  $\alpha_3$  decreases with elevating T. At  $T_s = 325$  °C, only one range of  $\ln \epsilon$  vs  $\ln t_s$  is drawn, so only one value could be recorded for  $\alpha$ .

It is found that  $\alpha$  increased with increasing T. At 400 °C, two values  $\alpha_1$  and  $\alpha_2$  could be recorded at each temperature. It is clear from table (8) that  $\alpha_1$  increased negatively with elevating T. Also,  $\alpha_2$  increased with elevating T.

**Table (8) :** Variation of  $\alpha$  with T and  $T_s$ .

T(K)	$\alpha_1$	$\alpha_2$	$\alpha_3$	$T_s(^{\circ}C)$
183	-0.00637	0.00827	0.000549	250
213	-0.00697	0.00916	0.000479	
243	-0.00788	0.01042	0.000396	
273	-0.00918	0.01217	0.000220	
303	-0.01082	0.01430	0.000072	
333	-0.01313	0.01727	-0.000280	
363	-0.01667	0.02196	-0.000919	
383	-0.02036	0.02690	-0.001550	
-----				
--				
183	0.00591	-----	-----	325
213	0.00614	-----	-----	
243	0.00686	-----	-----	
273	0.00812	-----	-----	
303	0.01045	-----	-----	
333	0.01307	-----	-----	
363	0.01732	-----	-----	
383	0.02161	-----	-----	
-----				
--				
183	-0.00974	0.02154	-----	400
213	-0.01072	0.02240	-----	
243	-0.01260	0.02412	-----	
273	-0.01507	0.02584	-----	
303	-0.01782	0.02767	-----	
333	-0.02210	0.03230	-----	
363	-0.02904	0.03752	-----	
383	-0.03620	0.04534	-----	

The obtained values for the power  $\alpha$  are not comparable with those known for the different mechanisms contribute to the processes of material transport due to the process of sintering using equation ;

$$\epsilon = C t^m \tag{14}$$

suggested by Johnson and Cutler [1963]. The discrepancy lie in, first, the power  $m$  does not possess minus sign except in case of dilation instead of shrinkage. Second, the values recorded for the power  $m$  in equ.(14) possess relatively high values compared with those obtained for  $\alpha$ . For the sake of reminiscence, the value of  $m$  depends mainly on the process of material transport and filling the pores between the particles and depends also on the contact between the initial grains. First of all, it has to be mentioned that, the prepared ternary is of a layer structure type and the role of filling the pores by transport materials from the original grain is wether absent or at least very weak. Therefore, contribution to the change in resistivity with the time of sintering can be considered to be mainly due to, formation of chemical bonds especially in case of the metallic behaviour and intergrain or intragrain hopping especially in case of semiconductor behaviour. However, it is believed that, the shape of the grain boundaries and link strength between the grains and the grain boundary distribution can contribute to a dominant role. The sign of  $\alpha$  being plus or minus, reveals wether  $\rho_s$  increases or decreases with prolongating  $t_s$ . It is a matter depends on the consequence of the contribution of the above mentioned parameters to  $\rho_s$ .

## 5. Conclusion:

Because of both semimetallic and semiconductor behaviour which could be observed together in a certain compact depending on the conditions of sintering, the electrical conductivity could not be enhanced thermally at all. However, as for many different semiconducting chalcogenides whether in bulk or thin films form, the electrical conductivity showed an enhancement by the electric field within the intermediate range of the latter. Similar results could be observed formerly for similar chalcogenides, Marshal and Miller [1973]. Within this range of field enhancement of the electrical conductivity, Marshal and Miller model seemed applicable. Accordingly, equ.(1) was used to calculate both characteristic length  $a(T)$  and the zero – field conductivity  $\sigma(0,T)$ . However, it was found that the parameters are dependent on the environmental temperature through the power of eqs.(2,3). However, most of the temperature enhancement of the zero – field conductivity was attributed to a corresponding enhancement in the charge carrier concentration. On the other hand, the charactristic length was found to be also enhancing with  $T$ . That is because of the enhancement of the scattering processes by temperature.

Where the behavior was semimetallic which is familiar for such chalcogenides containing Pb or Sn, Kulbachinskii et al[1994], the temperature dependence of resistivity could be described by the power eq.(6). The values of both the power and the residual resistivity could be calculated. However, the

values of the power of eq.(6) were found to be  $< 1$  indicating strong deviation from the behavior of normal metals in such elevated range of T

Where the behavior was that of semiconductors, the values obtained for conduction activation energy were found to be very small confirming weak dependence of resistivity on temperature. This recommended the thought of the hopping mechanism to conduction. Thence, the model proposed by Mott[1971] was applied and the different corresponding parameters were calculated. Despite, the compacts were all prepared at the same conditions, the Mott parameters did not possess equal values for all compacts indicating that the sampling effect can not be ignored in case of physical powder metallurgy studies. The characteristic temperature  $T_0$  and the temperature independent conductivity  $\sigma_0$  were found to increase from one lower to the successive higher stage of dependence of the hopping conductivity on temperature. This reveals that, the hopping conduction is thermally assisted type. In contrast, for green compacts,  $N(E_F)$  was found to decrease with elevating the range of T which confirms the possibility of contribution of conduction in the extended states especially in the high range of T. The small values obtained for the hopping length confirm the domination of intragrain hopping, despite the role of intergrain hopping can not be ignored. The small values obtained for the hopping energy can be regarded to the small values obtained for the hopping length (easy hopping), however, both R and W in direct proportionality. Besides, the discrepancy between the values obtained for the hopping energy (W) and those obtained for  $\Delta E_{a(T)}$  confirms the contribution of both intergrain and intragrain hopping to the total hopping process of conduction. However, because of the different complicated factors influencing the product of the sintering process, there were no explicit roles to control the influence of both the time and temperature of sintering on the different Mott parameters.

The normalized change in resistivity with the time of sintering could be generalized in the eq.(13) at the three temperatures considered for sintering. Meanwhile, the power of eq.(13) was found to change sequentially with the temperature of measurement despite it seemed having the possibility wither minus or plus sign. However, the values obtained for the power of eq.(13) were not comparable with those known for the different mechanisms mechanisms contribute to material transport due to the process of sintering as suggested by Johnson and Cutler[1963]. The discrepancy attributed to the layer structure of the prepared ternary (Kulbachinskii et al [1997]) and so, the change in resistivity is not due to material transport but, the initiated chemical bond and both the inter and intragrain hopping can play the dominant roles of conduction.

**References**

1. Nimtz G., Schlicht B., and Dornhaus R., *Narrow Gap Semiconductors*, Springer, Berlin 1983.
2. Story T., *Acta Phys Pol. A* 92, 663(1997).
3. (Xi – Song Zhou, Yuan Deng, Ce – Wen Nan and Yuan Huo Lin. *Journal of alloys and compounds* volume 352 (2003) p328).
4. Situlina O. V., Glazov V. M. : *Akad. Nauk. SSSR Chem.* 167 (1969)587.
5. Massalski T. B., Okamoto H., Subramanian P. R. and Kacprzak L. : *Binary Alloys Phase Diagram* ( ASM international, Ohio, (1992) 2ed ed.
6. Rudolph R., Krgger H., Fellmuth B. and Herrmann R., *Phys. Status Solidi (b)*, 102, 295(1980).
7. Z. Zhang, X. Sun, M.S. Dresselhaus, J. Y. Ying and J. Heremans *J.Phys. Rev. B*61(200)p4850
8. Ibrahim M. M., *Indian Journal of Pure & Applied Physic* 18, 242(1980)
9. Birkholz U.: *Thermoelektrische Bauelemente*, in *Amorphe und polykristalline Halbleiter*, ed. W. HEYWANG, Berlin 1984.
10. Bates C. W. Jr and England L, *Appl Phys Lett*, 14(1969)390.
11. Ibrahim M. M., Afify N., Hafiz M. M. Mahmoud M. A., *Powder Metallurgy International* vol. 20, no. 6, (1988).
12. Yokota K., Katayama S.: *Effect of the Heat Treatment On The Electrical Properties Of Bi<sub>2</sub>Te<sub>3</sub>*. *Technology Reports Of Kansai University* (1975) [16].
13. Marshall, J.M. and Miller, J.R., *Phil. Mag.* 27, 1151(1973).
14. Kulbachinskii V. A., Inoue M., Sasaki M., Negishi H., Gao W. X., Takase K., and Gimán Y., *Phus. Rev. B* Vol. 50, No. 23(1994) 16921.
15. Mott N. F. : *Philos. Mag.* 24(1971)1.
16. Jonson D. L. and Cutler I. B., *J. Am. Ceram. Soc.*, 46, 541(1963).
17. Kulbachinskii V. A., Negishi H., Sasaki M., Gimán Y., Inoue M., Lostak P., and Horak J., *Phys. Stat. Soli.(b)* 199, 505(1997).